

Revisiting the “Fundamental Plane” of Black Hole Activity at Extremely Low Luminosities

Feng Yuan¹, Zhaolong Yu^{1,2}, and Luis C. Ho³

ABSTRACT

We investigate the origin of the X-ray emission in low-luminosity AGNs (LLAGNs). Yuan & Cui (2005) predicted that the X-ray emission should originate from jets rather than from an advection-dominated accretion flow (ADAF) when the X-ray luminosity L_X of the source is below a critical value of $L_{X,\text{crit}} \approx 10^{-6}L_{\text{Edd}}$. This prediction implies that the X-ray spectrum in such sources should be fitted by jets rather than ADAFs. Furthermore, below $L_{X,\text{crit}}$ the correlation between radio (L_R) and X-ray (L_X) luminosities and the black hole mass (M)—the so-called fundamental plane of black hole activity—should deviate from the general correlation obtained by Merloni, Heinz & Di Matteo (2003) and become steeper. The Merloni et al. correlation is described by $\log L_R = 0.6\log L_X + 0.78\log M + 7.33$, while the predicted correlation is $\log L_R = 1.23\log L_X + 0.25\log M - 13.45$. We collect data from the literature to check the validity of these two expectations. We find that among the 16 LLAGNs with good X-ray and radio spectra, 13 are consistent with the Yuan & Cui prediction. For the 22 LLAGNs with $L_X < L_{X,\text{crit}}$, the fundamental plane correlation is described by $\log L_R = 1.22\log L_X + 0.23\log M - 12.46$, also in excellent agreement with the prediction.

Subject headings: accretion, accretion disks — black hole physics — galaxies: active — quasars: general — X-rays: general

1. Introduction

Understanding the radiative quiescence of massive black holes has important implications for accretion physics, fueling and feedback mechanisms, and black hole growth over

¹Key Laboratory for Research in Galaxies and Cosmology, Shanghai Astronomical Observatory, Chinese Academy of Sciences, 80 Nandan Road, Shanghai 200030, China; fyuan@shao.ac.cn

²Graduate School of the Chinese Academy of Sciences, Beijing 100039, China

³The Observatories of the Carnegie Institution of Washington, 813 Santa Barbara Street, Pasadena, CA 91101, USA

cosmic time (Ho 2004; Pellegrini 2005). A viable physical model for the low luminosity of most nearby active galactic nuclei (AGNs) is widely believed to be due to the radiative inefficiency of advection-dominated accretion flows (ADAFs; Narayan & Yi 1994; 1995; see Ho 2008 for a review on observational evidence on this point) present in these systems. Moreover, the X-ray radiation of most low-luminosity AGNs (LLAGNs) is believed to originate from ADAFs (see Yuan 2007 for a review). LLAGNs are generally radio-loud (Ho 2008). The radio radiation of AGNs is under-predicted by ADAFs and is widely accepted to be from jets (e.g., Ho 2008 and references therein). Merloni et al. (2003; see also Falcke et al. 2004) find a so-called fundamental plane of black hole activity, which is a correlation between the black hole mass and radio and X-ray luminosities:

$$\log L_{\text{R}} = (0.6^{+0.11}_{-0.11})\log L_{\text{X}} + (0.78^{+0.11}_{-0.09})\log M + 7.33^{+4.05}_{-4.07}. \quad (1)$$

The unit of luminosity is erg s^{-1} , and the black hole mass M is in units of M_{\odot} . This finding is based on the radio-X-ray correlation of some black hole X-ray binaries found by Gallo et al. (2003) and Corbel et al. (2003) (but see Xue & Cui 2007). The scatter of the correlation, however, is quite large.

Yuan & Cui (2005; hereinafter YC05) successfully interpret this correlation based on an ADAF-jet model (to be described in §3). In this model, the X-ray radiation comes from the Comptonization process in ADAFs while the radio originates from synchrotron emission in jets. Obviously a key parameter here is the fraction of the accretion material that goes into the jet, $\dot{M}_{\text{jet}}/\dot{M}$. YC05 find that to explain the correlation requires $\dot{M}_{\text{jet}}/\dot{M} \approx \text{constant}$ for $\delta = 0.01$ and $\dot{M}_{\text{jet}}/\dot{M} \propto \dot{M}^{-0.5}$ for $\delta = 0.5$. Here, δ is a parameter in the ADAF model that describes the fraction of turbulent dissipation that directly heats the electrons (see Fig. 5 in YC05). Most of the sources in the sample of Merloni et al. (2003) are relatively luminous. By extrapolating the above \dot{M}_{jet} vs. \dot{M} relation to lower accretion rates, YC05 predict that the X-ray emission of the system should originate from jets rather than ADAFs when the X-ray luminosity in the 2–10 keV band, $L_{2-10\text{keV}}$, is lower than a critical value $L_{\text{X,crit}}$:

$$\log \left(\frac{L_{\text{X,crit}}}{L_{\text{Edd}}} \right) = -5.356 - 0.17 \log \left(\frac{M}{M_{\odot}} \right). \quad (2)$$

The physical reason is as follows. The X-ray emission from the ADAF is due to thermal Comptonization of the synchrotron photons in the ADAF, which is roughly proportional to \dot{M}^2 . The synchrotron emission from the jet is proportional to the density or the mass flux of the jet, \dot{M}_{jet} . For $\dot{M}_{\text{jet}} \propto \dot{M}$ or $\dot{M}_{\text{jet}} \propto \dot{M}^{0.5}$, as \dot{M} decreases, the synchrotron emission from the jet will catch up with the Comptonization emission from the ADAF and finally dominate the X-ray emission below a certain \dot{M} , which corresponds to $L_{\text{X,crit}}$ defined in eq. (2) above. YC05 predict that below $L_{\text{X,crit}}$ the correlation should correspondingly steepen

into the following form:

$$\log L_{\text{R}} = 1.23 \log L_{\text{X}} + 0.25 \log M - 13.45. \quad (3)$$

We would like to emphasize two points here. First, the work of YC05 is based on two assumptions: (1) that jets always exist in LLAGNs and (2) that the physics of the jet does not depend on the luminosity of the sources (it remains the same even when the luminosity becomes extremely low). Second, all the above-mentioned correlations, and the critical luminosity defined by eq. (2) hold only in statistical sense. Given the large scatter in the normalization of the primary fundamental plane relation (Merloni et al. 2003), it is possible that any individual source may not follow the correlation well, or that its critical luminosity may differ significantly from that described by eq. (2). For the sake of concreteness, throughout this paper we neglect this complication, although we should keep this in mind when we quantitatively assess observations. Note, however, that the slope of eq. (3) is not affected because it is determined only by jet physics.

Different from the above scenario, some people propose that the X-ray emission *always* comes from jets, irrelevant to the luminosities of the sources. Markoff et al. (2001) model the broadband spectrum of the relatively luminous hard state of XTE J1118+480 using a jet model. In this work, both the radio and X-ray emission come from the jet. Markoff et al. (2003) subsequently interpret the Merloni et al. correlation described by eq. (1) using this jet model. Note that, different from YC05, no break in the correlation is expected at lower luminosities in this model. In addition, the correlation spectral index between radio and X-ray is calculated to be ~ 0.6 , i.e., consistent with eq. (1). This is again different from YC05 (see also Heinz 2004), where when both radio and X-ray emission originate from a jet, the correlation spectral index is calculated to be ~ 1.23 (see eq. 3). As Heinz (2004) points out, and confirmed later in YC05, the discrepancy arises because Markoff et al. do not take into account the cooling effect in the electron's steady energy distribution.

The validity of the prediction of YC05 can be checked in two ways. The first is by modeling the X-ray spectra of sources with X-ray luminosities $L_{\text{X}} < L_{\text{X,crit}}$. In the usual $\log(\nu L_{\nu})$ vs. $\log \nu$ spectral plot, if the X-ray spectrum originates from a jet, it forms a straight line (i.e., a power-law spectrum); if, on the other hand, it originates from an ADAF, the spectrum should be curved. Wu et al. (2007) model eight FR I sources using a coupled jet-ADAF model. The X-ray luminosities of these sources are usually low, $L_{\text{X}}/L_{\text{Edd}} \approx 10^{-4} - 10^{-8}$. They find that the X-ray emission in the brightest source ($L_{\text{X}}/L_{\text{Edd}} \approx 1.8 \times 10^{-4}$) is from an ADAF. The results for the four sources with moderate luminosities are complicated, with two being dominated by an ADAF, one by jets, and the other fitted by a combination of the two. The X-ray emission of the three least luminous sources is dominated by a jet. Modeling data from deep *XMM-Newton* observations of two black hole transients in

quiescence, Pszota et al. (2008) find that the X-ray spectra are of power-law shape. These spectra are expected if the jet dominates the X-ray emission, but they deviate significantly from the expected spectrum of an ADAF at very low \dot{M} .

The second way to check the YC05 prediction is to look at the radio-X-ray correlation. In this context, Pelligrini et al. (2007) present a multiwavelength study of the quiescent black hole in the elliptical galaxy NGC 821, combining radio data from the VLA and X-ray data from *Chandra*. This source is very dim, with $L_{2-10\text{keV}} \approx 10^{-8}L_{\text{Edd}} \ll L_{\text{X,crit}} \approx 2 \times 10^{-7}L_{\text{Edd}}$. They find that the source follows the correlation described by eq. (3) much more closely than that of eq. (2). Wrobel et al. (2008) analyze similar data for two additional quiescent black holes in the elliptical galaxies NGC 4621 and NGC 4697. For both sources, they find that the radio fluxes predicted by eq. (3) are in relatively good agreement (within a factor of 3) compared to the observed values. Wang et al. (2006) and Li et al. (2008) reinvestigate the fundamental plane relation using a significantly larger sample of AGNs selected from the Sloan Digital Sky Survey. They find that the correlation slope for radio-loud AGNs is 1.39, steeper than the slope of 0.85 for the radio-quiet AGNs. Since in radio-loud AGNs essentially all of the radio emission and a significant fraction of the X-ray emission come from jets, whereas in radio-quiet sources the X-ray emission is dominated by the accretion flow, the steeper slope found for radio-loud AGNs is qualitatively consistent with the prediction of YC05. However, obviously more direct data for sources with $L_{\text{X}} < L_{\text{X,crit}}$ would be highly desirable.

In the present paper, we collect data from the literature to check the prediction of YC05. We use a new sample of 22 LLAGNs with well-measured black hole masses and radio and X-ray luminosities (Table 1) to reexamine the fundamental plane correlation in the regime $L_{\text{X}} < L_{\text{X,crit}}$ (§3). In a complementary approach, we then model the spectral energy distributions of another set of sources (Table 2) using an accretion-jet model to investigate the origin of the X-ray emission (§4). Section 5 summarizes our main conclusions.

2. The “Fundamental Plane” of Black Hole Activity at Extremely Low Luminosity

To examine whether LLAGNs follow the correlations described by eq. (1) or eq. (3), we collect black hole masses, radio (5 GHz) luminosities, and X-ray (2–10 keV) luminosities for sources with $L_{\text{X}} < L_{\text{X,crit}}$. We find 22 sources that meet this criterion (Table 1), as shown by the left plot of Figure 1. We do not include Sgr A*, even though its luminosity satisfies our criterion. This is because current observations indicate that there is no jet in this source, and thus it violates the assumption of YC05. Within our sample, seven sources (namely

M 31, M 32, NGC 1399, NGC 3675, NGC 4472, NGC 4494, and NGC 4636) only have upper limits for their radio or X-ray luminosities. For three sources (NGC 404, NGC 4621, and NGC 4697), we only have radio luminosities at frequencies other than 5 GHz. For these objects we deduce the luminosity at 5 GHz either by extrapolating the observed radio spectrum (NGC 404) or, when no radio spectrum is available (NGC 4621 and NGC 4697), by assuming the radio spectrum predicted by our jet model.

We use the approach adopted by Merloni et al. (2003) and Wang et al. (2006) to analyze the correlation between radio and X-ray luminosities and the black hole mass. The solid line in the left plot of Figure 1 shows the best fit to all the 22 sources. It is described by

$$\log L_{\text{R}} = 1.22(\pm 0.02)\log L_{\text{X}} + 0.23(\pm 0.03)\log M - 12.46. \quad (4)$$

If we exclude the seven sources with upper limits, the correlation for the remaining 15 sources is shown by the solid line in the right plot of Figure 1. It is described by

$$\log L_{\text{R}} = 1.29(\pm 0.03)\log L_{\text{X}} + 0.11(\pm 0.04)\log M - 14.1. \quad (5)$$

The above results clearly indicate that for sources with $L_{\text{X}} < L_{\text{X,crit}}$ the correlation index between L_{X} and L_{R} is in much better agreement with the prediction of YC05 than Merloni et al. (2003).

3. The ADAF-Jet Model

We briefly describe the ADAF-jet model here. The readers can refer to Yuan et al. (2005) for additional details.

3.1. The ADAF Model

The accretion flow consists of two parts. Within a “transition” radius R_{out} the flow is described by an ADAF (sometimes also called a “radiatively inefficient accretion flow”; Narayan & Yi 1994, 1995). Outside of R_{out} , the accretion flow is described by a standard thin disk. Both observations and theoretical studies indicate that the value of this radius is a function of accretion rate (Liu et al. 1999; Meyer et al. 2000; Yuan & Narayan 2004). Numerical simulations (Stone et al. 1999; Hawley & Balbus 2002; Igumenshchev et al. 2003) and analytical work (Narayan & Yi 1994; Blandford & Begelman 1999; Narayan et al. 2000; Quataert & Gruzinov 2000) on ADAFs indicate that only a fraction of the gas available at large radius actually accretes onto the black hole. The rest of the gas is either ejected from the

flow or is prevented from being accreted by convective motions. We therefore parameterize the accretion rate with a parameter s , defined such that $\dot{M} = \dot{M}_{\text{out}}(R/R_{\text{out}})^s$, where \dot{M}_{out} is the accretion rate at the boundary R_{out} . There is obviously a degeneracy between \dot{M}_{out} and s when the accretion rate at the innermost region of the ADAF is concerned. We calculate the global dynamical solution of the ADAF. Other parameters include the viscosity parameter α and magnetic parameter β [defined as the ratio of the gas to the total pressure (sum of gas and magnetic pressure) in the accretion flow, $\beta = P_g/P_{\text{tot}}$], and δ , the fraction of the turbulent dissipation that directly heats the electrons. The radiative processes we consider include synchrotron, bremsstrahlung, and their Comptonization. After the ADAF structure is obtained, the spectrum of the flow can be calculated in the same way as in previous work (e.g., Yuan et al. 2003). Specifically, the X-ray radiation comes from the thermal Comptonization process.

In our calculation we adopt typical values of $\alpha = 0.3$ and $\beta = 0.9$, which are widely used in ADAF models. Although these two values are still not well constrained and some uncertainties still exist, their values do not significantly affect the X-ray spectrum. This is partly because their effects are absorbed in \dot{M}_{out} and δ , respectively. The main parameter left in the ADAF model is therefore δ . The value of the parameter δ (and also s) are well constrained in the case of our Galactic center black hole, Sgr A* (Yuan et al. 2003). Assuming that the physics of the ADAFs is the same for various objects, we thus follow Yuan et al. (2003) and adopt $\delta = 0.5$ and $s = 0.3$ as “fiducial” values. But we also try other values if we cannot get a good fit to the observations. In summary, the X-ray spectrum, including the normalization and the spectral slope, which is what concern us mostly in the present work, is mainly determined by the combination of the accretion rate at the innermost region of the ADAF (which is determined by the combination of \dot{M}_{out} , R_{out} , and s) and the electron temperature (which is determined mainly by δ). Roughly speaking, there is a one-to-one correspondance between the normalization and the spectral slope, and the photon index predicted by an ADAF in the 2–10 keV band ranges from $\Gamma \lesssim 1.5$ at the highest luminosities to $\Gamma \gtrsim 2$ at the lowest luminosities (see, e.g., Fig. 3a in Esin et al. 1997).

3.2. The Jet Model

The jet model adopted in the present paper is based on the internal shock scenario, which has also been widely used in the study of gamma-ray burst afterglows. A fraction of the material in the accretion flow is assumed to be transferred into the vertical direction to form a jet. The mass lost rate is set as \dot{M}_{jet} . The jet is assumed to have a conical geometry with half-open angle ϕ and bulk Lorentz factor Γ_{jet} . Throughout this paper we generally

assume $\phi = 0.1$ and $\Gamma_{\text{jet}} = 10$ if there is no observational constraint on them. Internal shocks occur as a result of the collision between shells with different velocities. As a result, a small fraction of the electrons in the jet are accelerated into a power-law energy distribution with index p . Shock acceleration theory typically gives $3 > p > 2$. For example, for relativistic shocks in Bednarz & Ostrowski (1998) and Kirk et al. (2000) obtain $p \approx 2.2$. However, there is still some uncertainty in our understanding of shock acceleration, and, more generally, the acceleration mechanism of electrons in jets; for instance, magnetic reconnection may be another relevant mechanism in addition to shocks. So we also try values of $p < 2$. In this context, we note that the modeling of BL Lac objects, where the emission comes from predominantly from jets, sometimes also requires $p < 2$ (e.g., Ghisellini et al. 2002). We assume that the fraction of accelerated electrons is ξ_e and fix $\xi_e = 1\%$ in our calculations. The energy density of accelerated electrons and amplified magnetic field in the shock front are described by two free parameters ϵ_e and ϵ_B . Medvedev (2006) shows that they should roughly follow $\epsilon_e \sim \epsilon_B^{1/2}$.

Only synchrotron emission is considered in the calculation of the jet spectrum. Compton scattering is neglected. This approximation is suitable, as shown in Wu et al. (2007), when \dot{M}_{jet} is small, as is the case for all sources in the present work. This is because, on the one hand, when \dot{M}_{jet} is small, the ratio of the photon energy density to the magnetic field energy density is very low. Thus, the power of synchrotron self-Compton emission in the jet is several orders of magnitude less than that of synchrotron emission. On the other hand, $p \approx 2$ implies that a significant fraction of the synchrotron emission power lies in the X-ray band of our interest. The radio spectrum emitted by the jet is due to self-absorbed synchrotron emission from different parts of the jet, and the spectrum is usually flat (i.e., $\alpha \approx 0$, where $F_\nu \propto \nu^\alpha$). The X-ray emission comes from optically thin synchrotron emission from accelerated electrons in the jet, and the slope is mainly determined by the value of p . Since the radiative cooling timescale of these electrons is typically much shorter than the dynamical timescale, the spectral index of the *steady* distribution of electrons is $p + 1$. So the spectral index of the X-ray spectrum is $\alpha = -(p + 1 - 1)/2$, or $\alpha \approx -1$ for $p \approx 2$. The normalization of the spectrum is mainly determined by the values of ϵ_e and ϵ_B .

3.3. The Truncated Thin Disk

We do not consider the contribution to the spectral energy distribution from a truncated standard thin disk outside of R_{out} . The main reason is that we want to focus on the origin of the X-ray emission. For this purpose, only the jet and ADAF are the most relevant since the radiation of the standard thin disk only contributes up to the optical and ultraviolet

(UV) bands. For some sources in our sample, we do not have reliable data in the optical or UV. Good data at optical and UV, of course, can present additional constraints on the model parameters, but mainly to the combination of R_{out} and \dot{M}_{out} . As we describe before, there is a degeneracy between these two parameters when we model the X-ray emission from an ADAF, and so the constraint from the optical and UV data to the focus of our paper is very limited. For these reasons, we only consider the jet and ADAF components and only attempt to fit the radio and X-ray spectra.

4. Modeling Results for Individual Objects

We fit the radio and X-ray spectra of 16 sources using the ADAF-jet model. The results are shown in Figures 2 and 3, and the model parameters are listed in Table 2. The accretion rate of the ADAF and the mass loss rate of the jet are in unit of $\dot{M}_{\text{Edd}} \equiv 10L_{\text{Edd}}/c^2$. Among these sources, seven are dominated by ADAFs (Fig. 2) and nine by jets (Fig. 3). Regarding the origin of the X-ray emission, all but three of these 16 sources are consistent with the prediction of YC05. We describe the fitting results below.

4.1. ADAF-Dominated Sources

This type of sources includes IC 4296, NGC 315, NGC 1052, NGC 4203, NGC 4261, NGC 4579, and NGC 6251 (Fig. 2). The X-ray spectra of these sources can be fitted very well by ADAFs, while the contribution from jets is negligible. From Table 2, we see that for all these seven sources $L_{2-10\text{keV}} \gg L_{\text{X,crit}}$. This is consistent with the prediction of YC05. Below are notes to some sources.

IC 4296. The 0.3–10 keV X-ray spectrum of this source consists of two components, a power law that dominates above 1 keV with photon index $\Gamma = 1.48_{-0.34}^{+0.42}$ and soft thermal emission with $kT = 0.56_{-0.03}^{+0.03}$ keV that dominates below 1 keV. Since the thermal component likely comes from the host galaxy background, we only adopt the hard power-law component. The accretion rate required in our model is roughly consistent with the Bondi accretion rate derived by Pellegrini et al. (2003).

NGC 315. Worrall et al. (2007) obtained X-ray spectra of both the jet and the nucleus. The power-law component of the nucleus is described by $\Gamma = 1.57 \pm 0.11$, much harder than that of the jet, which is $\Gamma = 2.2 \pm 0.2$. The X-ray luminosity $L_{2-10\text{keV}} = 6 \times 10^{41} \text{ erg s}^{-1} \approx 1.5 \times 10^{-5} L_{\text{Edd}}$, which is much higher than the critical luminosity of $L_{\text{X,crit}} \approx 1.6 \times 10^{-7} L_{\text{Edd}}$. Worrall et al. (2007) argue that the X-rays from the jet must have a synchrotron origin,

which implies that the power-law index of the electrons is $p = 2.4 \pm 0.4$. The significant difference between the spectrum of the nucleus and the jet can be considered as possible evidence that the origin of the X-ray emission of the nucleus is from the accretion flow rather than from the jet. We see from the figure that this is consistent with our conclusion.

NGC 4261. From analysis of the *Chandra* image, the X-ray jet extends to the nucleus. Zezas et al. (2005) find that the X-ray spectrum can be well fitted by three components, namely a thermal component and two power laws with $\Gamma_1 = 1.54_{-0.39}^{+0.71}$ and $\Gamma_2 = 2.25_{-0.28}^{+0.52}$. Since the soft X-rays are dominated by the thermal component, we only adopt the data of the two power-law components, with the harder component being the dominant one. As shown in the figure, our modeling indicates that the dominant harder component comes from the ADAF while the softer one comes from the jet (Worrall & Birkinshaw 1994; Zezas et al. 2005), consistent with the prediction of YC05. This interpretation is consistent with the much lower absorption of the softer power-law component, $N_{\text{H}} < 3.7 \times 10^{20} \text{ cm}^{-2}$. Zezas et al. (2005) point out that this is also supported by the 1 keV flux of this component, which is within a factor of a few of that estimated on the basis of the nuclear 4.8 GHz radio flux, using the X-ray to radio ratio of knot A in the western jet.

NGC 4579. Quataert et al. (1999) have already modeled this source. They find that the X-ray spectrum can be fitted by the ADAF very well. Our calculation is in good agreement with theirs, as shown in the figure.

NGC 6251. Both *Chandra* and *XMM-Newton* observed this source (Evans et al. 2005). The spectra obtained appear to be mildly discrepant, given the formally quoted error bars. *Chandra* gives $\Gamma = 1.67 \pm 0.06$ while *XMM-Newton* gives a steeper spectrum with $\Gamma = 1.88 \pm 0.01$. The reason for the discrepancy is either genuine spectral variability or possibly residual photon pileup effects suffered by the *Chandra* data. We therefore only fit the *XMM-Newton* data.

4.2. Jet-Dominated Sources

This type of sources includes IC 1459, M 32, M 81, M 84, M 87, NGC 3998, NGC 4594, NGC 4621, and NGC 4697 (Fig. 3). The X-ray spectra (and radio, of course) of these sources can be fitted very well by jets, but not by the ADAF model. To illustrate this point, we show in the figure by the dot-dashed lines the emitted spectra from an ADAF. For M 32, M 81, M 84, M 87, NGC 3998, and NGC 4594, the parameters of the ADAF are adjusted so that the model can produce the “correct” X-ray flux. For the other three sources, the parameters of the ADAF are adjusted so that the model does not violate the radio data. From Table

2, we see that for all sources except IC 1459, M 81, and NGC 3998, $L_{2-10\text{keV}} \ll L_{X,\text{crit}}$. Consistent with the prediction of YC05, the X-ray emission is produced by jets. For the three outliers, $L_{2-10\text{keV}} > L_{X,\text{crit}}$. However, as we emphasize in §1, there is a large error bar in the value of $L_{X,\text{crit}}$ described by eq. (2). In addition, $L_{2-10\text{keV}}$ of these three sources are also not much different from $L_{X,\text{crit}}$ predicted by eq. (2) (ref. Table 2). Given the ill-defined errors on the actual measurements and the known large scatter in the normalization of the fundamental plane relation (and hence in the predicted value of $L_{X,\text{crit}}$), the exact value of $L_X/L_{X,\text{crit}}$ for any particular source should not be interpreted too literally. Below are notes to some sources.

IC 1459. The X-ray emission is well fitted by a jet, while the contribution of the ADAF is constrained by the radio data to be at very low level. Given that $L_{2-10\text{keV}} > L_{X,\text{crit}}$, the origin of X-ray emission is apparently inconsistent with the prediction of YC05, but, as mentioned above, we should be wary about overinterpretation of individual sources, especially in this case where $L_X/L_{X,\text{crit}}$ is only marginally greater than unity. The value of p is 1.9, formally but not significantly smaller than 2. Fabbiano et al. (2003) also fit the X-ray spectrum with a jet model, but with a much larger $p = 2.78$. The discrepancy of the value of p is because that they do not consider the effect of radiative cooling on the energy distribution of electrons. In another words, the value of p adopted there is the spectral index of the *steady* distribution rather than the *injected* distribution.

M 32. The X-ray spectrum is well fitted by a jet. The dot-dashed line shows our best fit by an ADAF; the fit is only marginally acceptable. However, the required accretion rate at the Bondi radius is $\sim 8 \times 10^{-6} M_\odot \text{ yr}^{-1}$, which is about 10 times larger than the Bondi rate $\dot{M}_{\text{Bondi}} \approx (3 - 10) \times 10^{-7} M_\odot \text{ yr}^{-1}$ estimated by Ho et al. (2003) from *Chandra* observations. This situation is very similar to the cases of M 31 and the quiescent state of the black hole X-ray binary XTE J1118+480 (YC05). In the case of M 31, Garcia et al. (2005) estimated the Bondi accretion rate from *Chandra* observations to be $\dot{M}_{\text{Bondi}} \approx 6 \times 10^{-6} \dot{M}_{\text{Edd}}$. However, the X-ray luminosity produced by an ADAF with such an accretion rate would be 4 orders of magnitude lower than the observed L_X . For XTE J1118+480, from optical observations together with disk instability theory for the outburst, the mass accretion rate is estimated to be $\dot{M} \approx 10^{-6} \dot{M}_{\text{Edd}}$ (McClintock et al. 2003). Again, an ADAF with such an accretion rate would underpredict the X-ray luminosity by nearly 4 orders of magnitude (YC05). If the X-ray radiation is dominated by a jet, on the other hand, this will not be a problem at all. Taking M 32 as an example, the mass accretion rate at the innermost region of the ADAF, say at $5R_S$, is about $\dot{M}_{\text{Bondi}}(5R_S/R_{\text{Bondi}})^{0.3} \approx 6 \times 10^{-7} \dot{M}_{\text{Edd}}$. So we only require $10^{-8}/6 \times 10^{-7} \approx 2\%$ of the accretion matter transferred into the jet to produce the correct X-ray flux. The physical reason is that the radiative efficiency of the jet is much higher than that of an ADAF.

M 81. We cannot model the X-ray emission using an ADAF component alone. In contrast to our result, Quataert et al. (1999) can fit the X-ray spectrum with an ADAF. The reason for the discrepancy is that the mass of the black hole they adopt is ~ 20 times smaller than ours. On the other hand, the X-ray spectrum is well fitted by the jet (see also Markoff et al. 2008), although the value of p in the jet model (1.8) is again formally smaller than 2.

M 87. The spectra of the nucleus and jet knots are very similar, and the X-ray flux of the knots closest to the nucleus is high. Wilson & Yang (2002) therefore suggest that the X-ray emission of the nucleus actually comes from the jet rather than the accretion flow. Our detailed modeling confirms their speculation. As shown in the figure, the X-ray spectrum is well fitted by the jet, but not by an ADAF. Di Matteo et al. (2003), on the other hand, were able to fit the X-ray spectrum with an ADAF. This is because they do not consider the outflow in their ADAF model.

NGC 3998. We find that it is hard to model the X-ray emission using an ADAF with outflow because the predicted spectrum of an ADAF is too hard. This conclusion is the same as in Ptak et al. (2004). If we abandon the requirement of significant outflow and direct electron heating (i.e. $\delta \ll 1$), we can fit the X-ray spectrum well, as in Ptak et al. (2004). But this kind of ADAF model is not favored from a theoretical point of view. On the other hand, a jet alone can fit the X-ray spectrum well, although we again require $p < 2$ (1.8).

NGC 4621. The X-ray luminosity of this source is extremely low. This makes the source suitable to test the prediction of YC05. As pointed out by Wrobel et al. (2008), application of the correlation of YC05 (eq. 3 above) predicts the observed radio flux to be $\nu L_\nu(8.5 \text{ GHz}) = 1.5 \times 10^{35} \text{ erg s}^{-1}$, which is in very good agreement with the observed value of $\nu L_\nu(8.5 \text{ GHz}) = 3.3 \times 10^{35} \text{ erg s}^{-1}$.

NGC 4697. This is another good source to test the prediction of YC05 since the luminosity is again extremely low. Consistent with YC05, the X-ray spectrum is fitted very well by a jet. Like NGC 4621, the application of the correlation of YC05 (eq. 3 above) predicts the observed radio flux to be $\nu L_\nu(8.5 \text{ GHz}) = 3.5 \times 10^{35} \text{ erg s}^{-1}$, which agrees well with the observed value of $\nu L_\nu(8.5 \text{ GHz}) = 1.3 \times 10^{35} \text{ erg s}^{-1}$, as pointed out by Wrobel et al. (2008).

5. Summary and Discussion

We collect data for a sample of LLAGNs to investigate the origin of their X-ray emission. YC05 predict that when the 2 – 10 keV luminosity of the system is smaller than a critical

luminosity $L_{X,\text{crit}}$ (see eq. (2) for its definition), the X-ray radiation will be dominated by the jet rather than by the ADAF. In this case, YC05 predict that the correlation between the mass of the black hole and the X-ray and radio luminosities will have a relation described by eq. (3), which is steeper than the correlation found by Merloni et al. (2003; eq. 1). In this paper we examine the validity of this prediction. We assemble black hole masses, radio luminosities, and X-ray luminosities for 22 sources from the literature with $L_{2-10\text{keV}} < L_{X,\text{crit}}$ to investigate their correlation. We find that the correlation is best described by eq. (4), which is very close to eq. (3) but much steeper than eq. (1). We also use our ADAF-jet model to fit the radio and X-ray spectral data of 16 sources covering a wider range in $L_{2-10\text{keV}}/L_{X,\text{crit}}$. We find that 13 sources are consistent with the prediction of YC05.

Fender et al. (2003) argue for a “jet-dominated” quiescent state in accreting black hole systems, in the sense that the kinetic power of the jet is much greater than the X-ray luminosity of the accretion flow when the X-ray luminosity is below a certain critical value. The similarity between this work and YC05 is that both emphasize the importance of the jet when the system is very dim. However, these two works are also intrinsically different, as discussed in YC05. Fender et al. compare the unobservable quantity “jet power” with the observable “X-ray luminosity.” They do not address the origin of the X-ray radiation of the system.

There is a dichotomy in the observed properties of the X-ray nuclei of FR I and FR II radio galaxies (Evans et al. 2006). The X-ray spectrum of FR Is is usually unabsorbed, while that of FR IIs is associated with high absorption and (narrow) iron line emission. In addition, the average photon index of the FR Is presented in Evans et al. (2006) is $\Gamma \approx 2$, while that of FR IIs is $\Gamma \approx 1.7$. Evans et al. (2006) speculate that this dichotomy arises from the relative contributions of the jet and accretion-related emission, which depends on the total power of the source. In less luminous FR I sources, the X-rays come from the jet and are largely devoid of absorption from the torus. By contrast, in FR II sources the X-rays come from the accretion flow, which is at least partly obscured by the torus. The model of YC05 presents a natural theoretical explanation to the above-mentioned observations and speculations. This is because FR I sources usually have luminosities below $L_{X,\text{crit}}$ while FR IIs are much more luminous (see also Wu et al. 2007). In addition, from Figures 2 and 3, we see that the spectrum produced by an ADAF is usually harder than that of a jet. The latter predicts $\Gamma = 1 + (p + 1 - 1)/2 \approx 2$ if $p \approx 2$.

Gallo et al. (2006) obtained radio and X-ray data for the quiescent state of the black hole binary system A0620–00, which has $L_X \approx 10^{-8.5} L_{\text{Edd}} \ll L_{X,\text{crit}} \approx 10^{-5.5} L_{\text{Edd}}$. They find that this source lies on the extrapolation of the “general” radio-X-ray correlation, which is dominated by the sources V404 Cyg and GX 339–4. However, we need to be cautious

when we conclude that the above result is not consistent with the YC05 prediction. As pointed out by Wu et al. (2007) and Corbel et al. (2008), because of the large scatter in the “general” correlation, it is not appropriate to connect one data point from *one* source with the data of *other* sources. Unfortunately, data for the more luminous hard state of A0620–00 are unavailable, which hampers us to reach any reliable conclusion.

Corbel et al. (2008) obtained simultaneous radio and X-ray data for both the hard and quiescent states of V404 Cyg. They find that the radio-X-ray correlation holds from the hard state down to its quiescent state, although the correlation slope index is ~ 0.5 , which is smaller than the general value of $0.6 - 0.7$. However, V404 Cyg is the brightest quiescent state black hole system known (Tomsick et al. 2003). The X-ray luminosity Corbel et al. (2008) observed is $L_X \approx 8 \times 10^{32} \text{ erg s}^{-1} \approx 6 \times 10^{-7} L_{\text{Edd}}$. This is only 5 times smaller than the critical luminosity calculated from eq. (1), $L_{X,\text{crit}} \approx 3 \times 10^{-6} L_{\text{Edd}}$, and thus the deviation of the correlation from eq. (2) is not expected to be large. This fact, combined with the large uncertainty of the theoretical model, leads us to think that it is hard to make a robust conclusion.

In summary, current investigations indicate that the YC05 prediction holds for most sources, including AGNs (YC05; Wu et al. 2007; Pellegrini et al. 2007; Wrobel et al. 2008; this work) and black hole X-ray binaries (YC05; Pszota et al. 2008). Since the correlation only holds in a statistical sense, it is not surprising that we find some outliers.

We close by noting that our results have an interesting implication for galaxy evolution. Feedback from the central black hole is now widely believed to play an important role in galaxy formation (e.g., Croton et al. 2006). The kinetic power of the jet provides an important source of energy feedback, and it would be valuable if this parameter can be estimated from observations. If the black hole system is in its “quiescent” phase, with $L_X \lesssim L_{X,\text{crit}}$, as many nearby galaxies seem to be, we can estimate the jet power P_{jet} from L_X because the observed X-ray luminosity comes from jets. What we need to know for this purpose is the radiative efficiency of jets, which is defined as $\eta_{\text{jet}} \equiv L_X/P_{\text{jet}}$. Specifically, $L_X \approx \delta^3 L_{X,\text{int}}$ and $P_{\text{jet}} = \Gamma_{\text{jet}}^2 \dot{M}_{\text{jet}} c^2$. Here $L_{X,\text{int}}$ is the intrinsic luminosity emitted by the jet in its comoving frame, Γ_{jet} is the Lorentz factor of the bulk motion of the jet, and $\delta \equiv [\Gamma_{\text{jet}}(1 - \beta \cos\theta)]^{-1}$ is the Doppler factor of the jet. So we have $\eta_{\text{jet}} = \delta^3 L_{X,\text{int}}/\Gamma_{\text{jet}}^2 \dot{M}_{\text{jet}} c^2$. For $1/\Gamma_{\text{jet}} < \theta < 1$, $\delta \approx \Gamma_{\text{jet}} \theta^2$, and thus $\eta_{\text{jet}} = \Gamma_{\text{jet}} \theta^6 L_{\text{int}}/\dot{M}_{\text{jet}} c^2$. From our modeling of the sources listed in Table 2, we have

$$\eta_{\text{jet}} \approx 10^{-5} \frac{\Gamma_{\text{jet}}}{10} \left(\frac{\theta}{60^\circ} \right)^6. \quad (6)$$

Thus, the “intrinsic” radiative efficiency of the jet $\eta_0 \equiv L_{X,\text{int}}/\Gamma_{\text{jet}}^2 \dot{M}_{\text{jet}} c^2 \approx 10^{-4} (\Gamma_{\text{jet}}/10)^{-2}$. It is interesting to note that this is consistent with the value obtained by Celotti & Fabian

(1993) — $\eta_0 \approx 10^{-4.1 \pm 2.2}$ — from modeling of the parsec-scale jets based on VLBI observations.

This work was supported in part by the Natural Science Foundation of China (grants 10773024, 10833002, 10821302, and 10825314), Bairen Program of Chinese Academy of Sciences, and the National Basic Research Program of China (973 Program 2009CB824800). The research of L.C.H. was supported by the Carnegie Institution of Washington.

Table 1: Sample with $L_{2-10\text{keV}} < L_{X,\text{crit}}$ Used for the Fundamental Plane Analysis

Object	$\log M$	Ref.	$\log L_R$	Ref.	$\log L_{2-10\text{keV}}$	Ref.
(1)	(2)	(3)	(4)	(5)	(6)	(7)
3C 66B	8.8	16,39	40.0	16,40	41.0	16,39
3C 338	9.2	1	40.0	1	40.3	1
3C 449	8.4	16,39	39.1	16,41	40.5	16,39
B2 0755+37	8.9	16,39	40.7	16,38	41.8	16,39
M 31	7.5	12,32	< 32.6	12,35	35.7	13
M 32	6.4	3,21	< 33.3	3	36.0	3
M 84	9.2	1,2,20	38.6	1	39.3	1
M 87	9.5	4	38.5	6,30	40.5	9,10
NGC 404	5.3	4	33.5	4,24	36.7	5
NGC 821	7.9	11,31	35.4	11	38.3	11
NGC 1399	9.1	19	< 38.7	18	39.0	17
NGC 2787	7.6	27	37.2	37,43	38.4	14,44
NGC 2841	8.4	15,36	36.0	15,37	38.3	14,15
NGC 3627	7.3	15,36	35.8	15,37	37.6	14,15
NGC 3675	7.1	36	< 36.0	37	38.0	14
NGC 4278	9.2	45	37.9	37,46	40.0	46
NGC 4472	8.9	2	36.7	15,37,42	< 38.8	17
NGC 4494	7.7	36	< 35.65	37	38.9	14
NGC 4594	9	2,7,25	37.9	6,26	40.2	7
NGC 4621	8.4	8,27	35.1	8	37.8	8
NGC 4636	8.5	2	36.4	15,37	< 38.4	17
NGC 4697	8.2	2,8,29	35.0	8	37.3	8

Col.(1): Name of the object. Col. (2): Logarithm of the black hole mass (M_\odot). (4) Logarithm of the nuclear radio luminosity at 5 GHz (erg s^{-1}). Col. (6): Logarithm of the X-ray luminosity in the 2–10 keV band (erg s^{-1}).

REFERENCES: (1) Evans et al. 2006; (2) Pellegrini 2005; (3) Ho et al. 2003; (4) Maoz 2007; (5) Eracleous et al. 2002; (6) Ho 1999; (7) Pellegrini et al. 2003b; (8) Wrobel et al. 2008; (9) Wilson & Yang 2002; (10) Di Matteo et al. 2003; (11) Pellegrini et al. 2007; (12) Garcia et al. 2000; (13) Garcia et al. 2005; (14) Ho et al. 2001; (15) Merloni et al. 2003; (16) Wu et al. 2007; (17) Loewenstein et al. 2004; (18) Killeen et al. 1988; (19) Houghton et al. 2006; (20) Bower et al. 1998; (21) Verolme et al. 2002; (22) Tonry et al. 2001; (23) Karachentsev et al. 1996; (24) Nagar et al. 2000; (25) Kormendy et al. 1996; (26) Hummel et al. 1984; (27) Tremaine et al. 2002; (28) Ravindranath et al. 2002; (29) Gebhardt et al. 2003; (30) Pauliny-Toth et al. 1981; (31) Richstone et al. 2004; (32) Kormendy & Bender 1999; (33) Stanek & Garnavich 1998; (34) Macri et al. 2001; (35) Crane et al. 1992; (36) Barth et al. 2002; (37) Nagar et al. 2002; (38) Capetti et al. 2002; (39) Donato et al. 2004; (40) Giovannini et al. 2001; (41) Katz-Stone & Rudnick 1997; (42) Ho & Ulvestad 2001; (43) Ho 2002; (44) Terashima et al. 2002; (45) Magorrian et al. 1998; (46) Terashima & Wilson 2003.

Table 2. Modeling of Individual Objects

Object	$M(M_{\odot})$	$L_{2-10\text{keV}}(L_{\text{Edd}})$	$L_{\text{X,crit}}(L_{\text{Edd}})$	Ref.	\dot{m}_{out}	$R_{\text{out}}(r_g)$	\dot{m}_{jet}	Γ	θ ($^{\circ}$)	ϵ_e	ϵ_B	p	Origin of X-rays	Consistent with YC05?
(1)	(2)	(3)	(4)	(5)	(6)	(7)	(8)	(9)	(10)	(11)	(12)	(13)		
IC 1459	2×10^9	1.7×10^{-7}	1.2×10^{-7}	19,20	2×10^{-4}	2×10^4	7×10^{-7}	10	30	0.028	0.02	1.9	jet	no
IC 4296	1×10^9	1.3×10^{-6}	1.3×10^{-7}	1	1.1×10^{-3}	2×10^4	7×10^{-6}	10	60	0.2	0.02	2.1	ADAF	yes
M 32	2.5×10^6	3×10^{-9}	3.6×10^{-7}	4	4.5×10^{-4}	2×10^5	1×10^{-8}	10	40	0.28	0.01	2.5	jet	yes
M 81	7×10^7	2.3×10^{-6}	2×10^{-7}	3,13,14,21	2×10^{-3}	2×10^4	2.4×10^{-7}	10	25	0.25	0.02	1.8	jet	no
M 84	1.6×10^9	1.1×10^{-8}	1.2×10^{-7}	2	2.5×10^{-4}	4×10^4	8×10^{-7}	10	63	0.2	0.02	2.35	jet	yes
M 87	3.4×10^9	8.1×10^{-8}	1×10^{-7}	15,16,3	1×10^{-3}	1×10^5	1×10^{-8}	20	19	0.14	0.02	2.5	jet	yes
NGC 315	3.1×10^8	1.5×10^{-5}	1.6×10^{-7}	5,6	4×10^{-3}	2×10^4	7×10^{-6}	10	38	0.15	0.02	2.5	ADAF	yes
NGC 1052	1.26×10^8	5.9×10^{-6}	1.85×10^{-7}	3	1.5×10^{-3}	1×10^{4a}	8×10^{-5}	10	60	0.2	0.02	2.3	ADAF	yes
NGC 3998	7×10^8	3×10^{-6}	1.4×10^{-7}	3,7,22	6×10^{-4}	6×10^2	9.8×10^{-8}	10	20	0.2	0.02	1.8	jet	no
NGC 4203	1×10^7	1.85×10^{-5}	2.84×10^{-7}	8,3	6×10^{-3}	1×10^3	1.5×10^{-6}	10	25	0.1	0.02	2.2	ADAF	yes
NGC 4261	4.9×10^9	4×10^{-6}	1.5×10^{-7}	17	1.7×10^{-3}	2×10^4	5×10^{-6}	10	63	0.3	0.01	2.45	ADAF	yes
NGC 4579 ^a	4×10^6	3×10^{-4}	3.3×10^{-7}	9,8	2.3×10^{-2}	2×10^2	8×10^{-5}	10	60	0.2	0.02	2.3	ADAF	yes
NGC 4594	1×10^9	1.2×10^{-7}	1.3×10^{-7}	10,11,9	5×10^{-4}	2×10^4	4×10^{-7}	10	45	0.3	0.02	1.8	jet	yes
NGC 4621	2.7×10^8	1.9×10^{-9}	1.6×10^{-7}	12	6×10^{-6}	2×10^4	4×10^{-8}	10	60	0.5	0.02	2.3	jet	yes
NGC 4697	1.7×10^8	1×10^{-9}	1.76×10^{-7}	12	6×10^{-6}	2×10^4	3.5×10^{-8}	10	60	0.3	0.02	2.1	jet	yes
NGC 6251	6×10^8	5×10^{-5}	1.4×10^{-7}	18	1.8×10^{-2}	2×10^4	4×10^{-6}	10	30	0.2	0.02	2.4	ADAF	yes

Note. — Col. (1): Name of object. Col. (2): Mass of the black hole. Col. (3): Luminosity in the 2–10 keV band. Col. (4): Critical luminosity from eq. (2). Col. (5): References. Col. (6): Mass accretion rate at R_{out} . Col. (7): R_{out} . Col. (8): Mass lost rate in the jet. Col. (9): Lorentz factor of the jet. Col. (10): Viewing angle of the jet. Col. (11): Energy density of accelerated electrons. Col. (12): Energy density of amplified magnetic field. Col. (13): Spectral index of energy distribution of electrons.

^aFor this source, $s = 0.1$, i.e. $\dot{M} = \dot{M}_{\text{out}}(R/R_{\text{out}})^{0.1}$

References. — (1) Pellegrini et al. 2003a; (2) Pellegrini et al. 2005; (3) Maoz 2007; (4) Ho et al. 2003; (5) Worrall et al. 2007; (6) Gu et al. 2007; (7) Ptak et al. 2004; (8) Terashima et al. 2002; (9) Ho 1999; (10) Hummel et al. 1984; (11) Pellegrini et al. 2003b; (12) Wrobel et al. 2008; (13) Schödel et al. 2007; (14) Markoff et al. 2008; (15) Wilson & Yang 2002; (16) Evans et al. 2006; (17) Zezas et al. 2005; (18) Evans et al. 2005; (19) Fabbiano et al. 2003; (20) Trinchieri & McDowell 2003; (21) Pellegrini et al. 2000a; (22) Pellegrini et al. 2000b.

REFERENCES

- Barth, A. J., Ho, L. C., & Sargent, W. L. W. 2002, *AJ*, 124, 2607
- Bednarz, J., & Ostrowski, M. 1998, *Phys. Rev. Lett.*, 80, 3911
- Blandford, R. D., & Begelman, M. C. 1999, *MNRAS*, 301, L1
- Bower, G. A., et al. 1998, *ApJ*, 492, L111
- Capetti, A., Celotti, A., Chiaberge, M., de Ruiter, H. R., Fanti, R., Morganti, R., & Parma, P. 2002, *A&A*, 383, 104
- Cellotti, A., & Fabian, A. C. 1993, *MNRAS*, 264, 228
- Corbel, S., Koerding, E., & Kaaret, P. 2008, *MNRAS*, 389, 1697
- Corbel, S., Nowak, M. A., Fender, R. P., Tzioumis, A. K., & Markoff, S. 2003, *A&A*, 400, 1007
- Crane, P. C., Dickel, J. R., & Cowan, J. J. 1992, *ApJ*, 390, L9
- Croton, D. J., et al. 2006, *MNRAS*, 365, 11
- Di Matteo, T., Allen, S. W., Fabian, A. C., Wilson, A. S., & Young, A. J. 2003, *ApJ*, 582, 133
- Donato, D., Sambruna, R. M., & Gliozzi, M. 2004, *ApJ*, 617, 915
- Eracleous, M., Shields, J. C., Chartas, G., & Moran, E. C. 2002, *ApJ*, 565, 108
- Esin, A. A., McClintock, J. E., & Narayan, R. 1997, *ApJ*, 489, 865
- Evans, D. A., et al. 2005, *MNRAS*, 359, 363
- Evans, D. A., et al. 2006, *ApJ*, 642, 96
- Falcke, H., Koerding, E., & Markoff, S. 2004, *A&A*, 414, 895
- Fender, R. P., Gallo, E., & Jonker, P. G. 2003, *MNRAS*, 343, L99
- Gallo, E., Fender, R., Miller-Jones, J., Merloni, A., Jonker, P., Heinz, S., Maccarone, T., & van der Klis, M. 2006, *MNRAS*, 370, 1351
- Gallo, E., Fender, R. P., & Pooley, G. G. 2003, *MNRAS*, 344, 60

- Garcia, M. R., Murray, S. S., Primini, F. A., Forman, W. R., McClintock, J. E., & Jones, C. 2000, *ApJ*, 537, L23
- Garcia, M. R., Williams, B. F., Yuan, F., Kong, A. K. H., Primini, F. A., Barmby, P., Kaaret, P., Murray, S. S. 2005, *ApJ*, 632, 1042
- Gebhardt, K., et al. 2003, *ApJ*, 583, 92
- Ghisellini, G., Celotti, A., & Costamante, L. 2002, *A&A*, 386, 833
- Giovannini, G., Cotton, W. D., Feretti, L., Lara, L., & Venturi, T. 2001, *ApJ*, 552, 508
- Giozzi, M., Sambruna, R. M., & Brandt, W. N. 2003, *A&A*, 408, 949
- Gu, Q.-S., Huang, J.-S., Wilson, G., & Fazio, G. G. 2007, *ApJ*, 671, L105
- Hawley, J. F., & Balbus, S. A. 2002, *ApJ*, 573, 738
- Heinz, S. 2004, *MNRAS*, 355, 835
- Ho, L. C. 1999, *ApJ*, 516, 672
- Ho, L. C. 2002, *ApJ*, 564, 120
- Ho, L. C. 2008, *ARA&A*, 46, 475
- Ho, L. C., Terashima, Y., & Ulvestad, J. S. 2003, *ApJ*, 589, 783
- Ho, L. C., & Ulvestad, J. S. 2001, *ApJS*, 133, 77
- Ho, L. C., et al. 2001, *ApJ*, 549, L51
- Houghton, R. C. W., Magorrian, J., Sarzi, M., Thatte, N., Davies, R. L., & Krajnović, D. 2006, *MNRAS*, 367, 2
- Hummel, E., van der Hulst, J. M., & Dickey, J. M. 1984, *A&A*, 134, 207
- Igumenshchev, I. V., Narayan, R., & Abramowicz, M. A. 2003, *ApJ*, 592, 1042
- Karachentsev, I. D., et al. 2002, *A&A*, 389, 812
- Katz-Stone, D. M., & Rudnick, L. 1997, *ApJ*, 488, 146
- Killen, N. E. B., Bicknell, G. V., & Ekers, R. D. 1988, *ApJ*, 325, 180
- Kirk, J. G., Guthmann, A. W., Gallant, Y. A., & Achterberg, A. 2000, *ApJ*, 542, 235

- Kormendy, J., & Bender, R. 1999, *ApJ*, 522, 772
- Kormendy, J., et al. 1996, *ApJ*, 473, L91
- Li, Z., Wu, X., & Wang, R. 2008, *ApJ*, 688, 826
- Liu, B. F., Yuan, W., Meyer, F., Meyer-Hofmeister, E., & Xie, G. Z. 1999, *ApJ*, 527, L17
- Loewenstein, M., Mushotzky, R. F., Angelini, L., & Arnaud, K. A. 2004, *ApJ*, 555, L21
- Macri, L. M., et al. 2001, *ApJ*, 549, 721
- Magorrian, J., et al. 1998, *AJ*, 115, 2285
- Maoz, D. 2007, *MNRAS*, 377, 1696
- Maoz, D., Nagar, N. M., Falcke, H., & Wilson, A. S. 2005, *ApJ*, 625, 699
- Markoff, S., Falcke, H. & Fender, R. 2001, *A&A*, 372, L25
- Markoff, S., Nowak, M., Corbel, S., Fender, R. & Falcke, H. 2003, *A&A*, 397, 645
- Markoff, S., et al. 2008, *ApJ*, 681, 905
- McClintock, J. E., Narayan, R., Garcia, M. R., Orosz, J. A., Remillard, R. A., & Murray, S. S. 2003, *ApJ*, 593, 435
- Medvedev, M. 2006, *ApJ*, 651, L9
- Merloni, A., Heinz, S., & Di Matteo, T. 2003, *MNRAS*, 345, 1057
- Meyer, F., Liu, B. F., & Meyer-Hofmeister, E. 2000, *A&A*, 354, L67
- Nagar, N. M., Falcke, H., Wilson, A. S., & Ho, L. C. 2000, *ApJ*, 542, 186
- Nagar, N. M., Falcke, H., Wilson, A. S., & Ulvestad, J. S. 2002, *A&A*, 392, 53
- Narayan, R., Igumenshchev, I. V., & Abramowicz, M. A. 2000, *ApJ*, 539, 798
- Narayan, R., & Yi, I. 1994, *ApJ*, 428, L13
- Narayan, R., & Yi, I. 1995, *ApJ*, 444, 231
- Pauliny-Toth, I. I. K., Preuss, E., Witzel, A., Graham, D., Kellermann, K. I., Ronnang, B. 1981, *AJ*, 86, 371
- Pellegrini, S. 2005, *ApJ*, 624, 155

- Pellegrini, S., Baldi, A., Fabbiano, G., & Kim, D.-W. 2003b, *ApJ*, 597, 175
- Pellegrini, S., Cappi, M., Bassani, L., Della Ceca, R. & Palumbo, G. G. C. 2000b, *A&A*, 360, 878
- Pellegrini, S., Cappi, M., Bassani, L., Malaguti, G., Palumbo, G. G. C., & Persic, M. 2000a, *A&A*, 353, 447
- Pellegrini, S., Siemiginowska, A., Fabbiano, G., Elvis, M., Greenhill, L., Soria, R., Baldi, A., & Kim, D. W. 2007, *ApJ*, 667, 749
- Pellegrini, S., Venturi, T., Comastri, A., Fabbiano, G., Fiore, F., Vignali, C., Morganti, R., & Trinchieri, G. 2003a, *ApJ*, 585, 677
- Pszota, G., Zhang, H., Yuan, F., & Cui, W. 2008, *MNRAS*, 389, 423
- Ptak, A., Terashima, Y., Ho, L. C., & Quataert, E. 2004, *ApJ*, 606, 173
- Quataert, E., Di Matteo, T., Narayan, R., & Ho, L. C. 1999, *ApJ*, 525, L89
- Quataert, E., & Gruzinov, A. 2000, *ApJ*, 539, 809
- Ravindranath, S., Ho, L. C., & Filippenko, A. V. 2002, *ApJ*, 566, 801
- Richstone, D., et al. 2004, *astro-ph/0403257*
- Schödel, R., Krips, M., Markoff, S., Neri, R., & Eckart, A. 2007, *Å*, 463, 551
- Stanek, K. Z., & Garnavich, P. M. 1998, *ApJ*, 503, L131
- Stone, J. M., Pringle, J. E., & Begelman, M. C. 1999, *MNRAS*, 310, 1002
- Terashima, Y., Iyomoto, N., Ho, L. C., & Ptak, A. F. 2002, *ApJS*, 139, 1
- Terashima, Y., & Wilson, A. S. 2003, *ApJ*, 583, 145
- Tomsick, J. A., et al. 2003, *ApJ*, 597, L133
- Tonry, J., Dressler, A., Blakeslee, J. P., Ajhar, E. A., Fletcher, A. B., Luppino, G. A., Metzger, M. R., & Moore, C. B. 2001, *ApJ*, 546, 681
- Tremaine, S., et al. 2002, *ApJ*, 574, 740
- Verolme, E. K., et al. 2002, *MNRAS*, 335, 517
- Wang, R., Wu, X., & Kong, M. 2006, *ApJ*, 645, 890

- Wilson, A. S., & Yang, Y. 2002, *ApJ*, 586, 133
- Worrall, D. M., & Birkinshaw, M. 1994, *ApJ*, 427, 134
- Worrall, D. M., Birkinshaw, M., Laing, R. A., Cotton, W. D., & Bridle, A. H. 2007, *MNRAS*, 380, 2
- Wrobel, J. M., Terashima, Y., & Ho, L. C. 2008, *ApJ*, 675, 1041
- Wu, Q., Yuan, F., & Cao, X. 2007, *ApJ*, 669, 96
- Xue, Y., & Cui, W. 2007, *A&A*, 466, 1053
- Yuan, F. 2007, in *The Central Engine of Active Galactic Nuclei*, ed. L. C. Ho & J.-M. Wang (San Francisco: ASP), 95
- Yuan, F., & Cui, W. 2005, *ApJ*, 629, 408 (YC05)
- Yuan, F., Cui, W., & Narayan, R. 2005, *ApJ*, 620, 905
- Yuan, F., & Narayan, R. 2004, *ApJ*, 612, 724
- Yuan, F., Quataert, E., & Narayan, R. 2003, *ApJ*, 598, 301
- Zezas, A., Birkinshaw, M., Worrall, D. M., Peters, A., & Fabbiano, G. 2005, *ApJ*, 627, 711

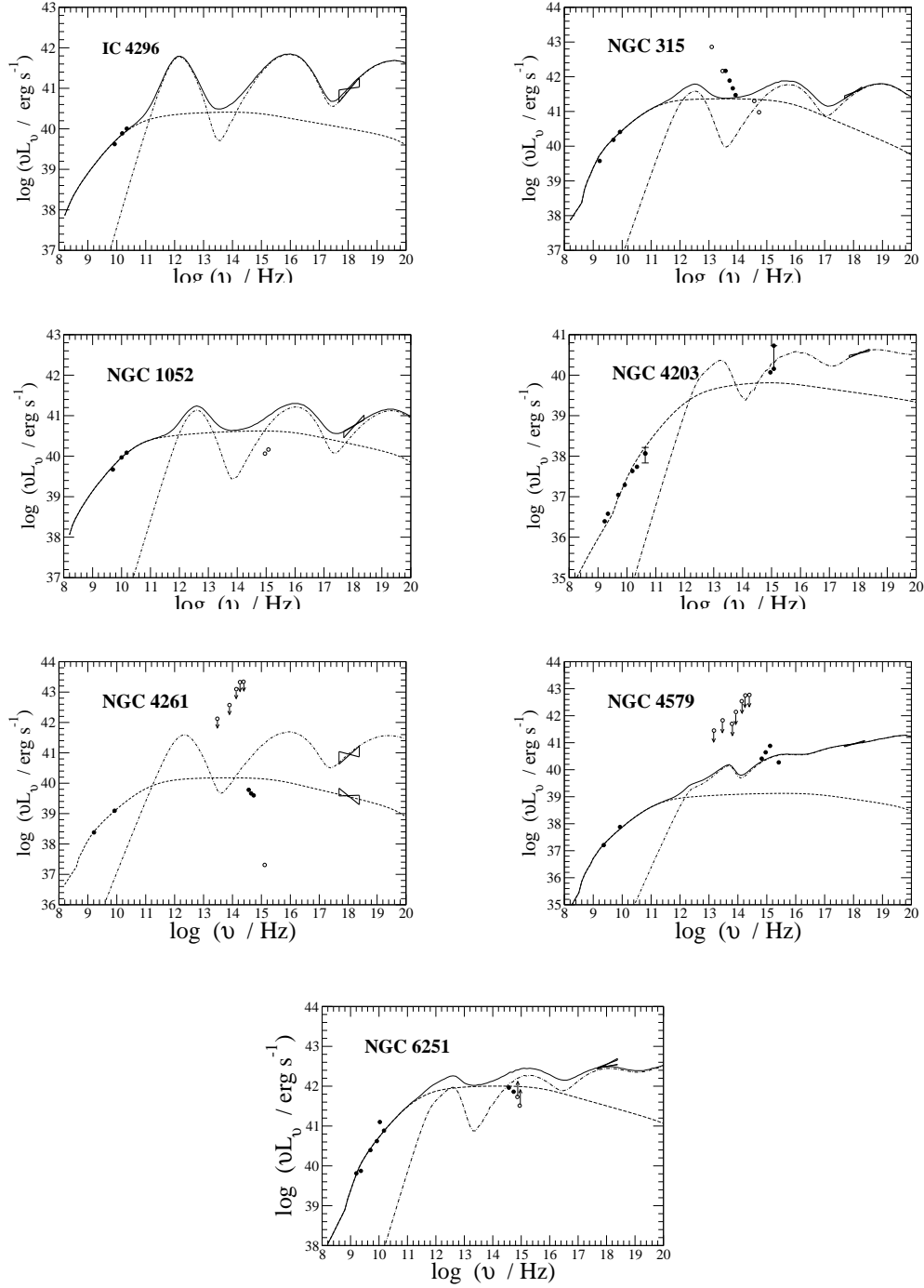


Fig. 2.— The ADADF-dominated sources. The dot-dashed lines show the emitted spectra of ADAFs, the dashed lines show the spectra of jets, and the solid lines show their sum. Reliable data points are plotted as solid symbols, whereas points severely affected by host galaxy contamination or extinction are plotted as open symbols. All of these sources are consistent with the prediction of YC05 (see Table 2).

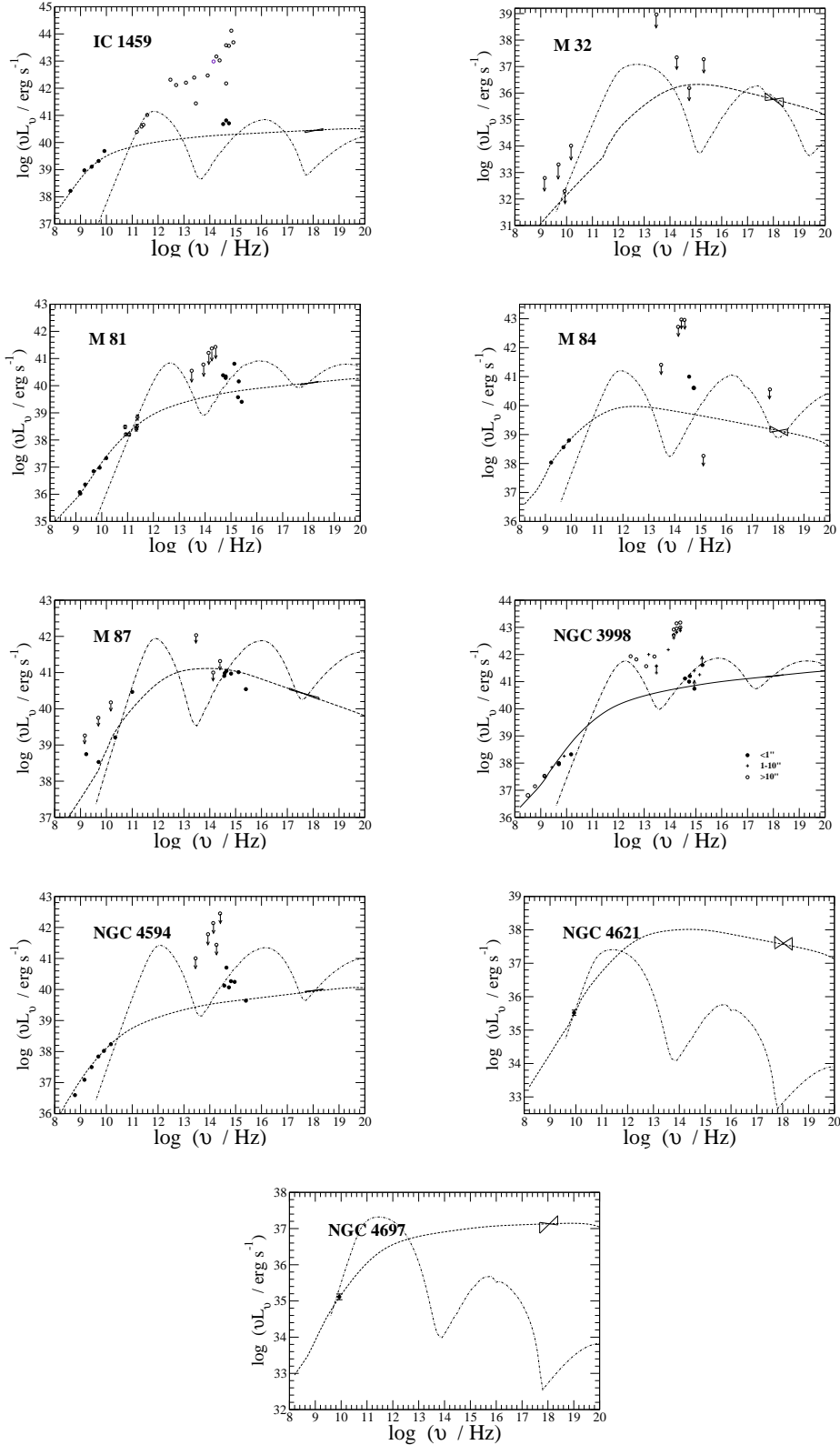


Fig. 3.— The jet-dominated sources. The dot-dashed lines show the emitted spectra of ADAFs, and the dashed lines show the spectra of jets. Reliable data points are plotted as solid symbols, whereas points severely affected by host galaxy contamination or extinction are plotted as open symbols. All of these sources, with the exception of IC 1459, M 81, and NGC 3998, are consistent with the prediction of YC05 (see Table 2)